Jet Stream-surface tracer relationships: Mechanism and sensitivity to source region

Gaige Hunter Kerr^{1*}, Darryn W. Waugh^{1,2}, and Scot M. Miller^{3,1}

¹Department of Earth and Planetary Sciences, Johns Hopkins University, Baltimore, Maryland, USA ²School of Mathematics and Statistics, University of New South Wales, Sydney, New South Wales,

Australia

 3 Department of Environmental Health and Engineering, Johns Hopkins University, Baltimore, Maryland,

USA

Key Points:

10

11

12

15

- The daily variability of near-surface tracer mixing ratios in the mid-latitudes is correlated with the latitude of the jet stream
- The sign of the jet-tracer relationships depends on the tracer source region and the resulting meridional tracer gradients
- The meridional movement of the jet stream alters the near-surface meridional flow, which changes tracer mixing ratios

Corresponding author: G. H. Kerr, ${\tt gaigekerr@gwu.edu}$

^{*}now at Department of Environmental and Occupational Health, George Washington University, Washington, DC, USA

Abstract

16

17

18

20

21

22

23

24

25

26

28

29

30

31

33

34

36

37

38

39

40

41

43

44

45

47

48

50

51

52

53

54

55

56

57

58

59

60

63

64

The daily variability of atmospheric trace gases stems from a combination of transport, chemistry, and emissions. Previous research has demonstrated the importance of the upperlevel jet stream on the variability of surface-level trace gases such as ozone (O_3) and carbon dioxide (CO₂), yet the cause of the daily variability and seasonal differences in the jet stream-trace gas relationship remain unclear. We test the possible drivers of this relationship using idealized tracers with different source regions within an atmospheric chemical transport model. The daily variability of all tracers is correlated with the meridional position of the jet stream in the mid-latitudes, but tracers emitted south of the jet increase in the mid-latitudes when the jet is poleward-shifted, while the opposite is true for tracers emitted at high latitudes. The jet stream regulates the near-surface meridional wind, and we find that this coupling together with the meridional tracer gradient can robustly predict regions where the jet stream and tracer mixing ratios are in and out of phase. This study elucidates the mechanisms underpinning a major driver of nearsurface trace gas variability and links these results with the location of emissions. Our results may be useful to inform future work focusing on jet-driven impacts to chemistryclimate connections.

Plain Language Summary

Previous studies have shown a connection between greenhouse gases or air pollutants and the jet stream, a narrow band of strong winds aloft that encircle the earth in the mid-latitudes. The mechanisms that connect the jet stream (generally 6-9 miles aloft) to changes in greenhouse gases and air pollutants at earth's surface are not well-recognized, and the ways which the location of pollutant and greenhouse gas emissions impact this relationship have been rarely quantified. To address these, we use computer models of the atmosphere that include "tracers," artificial particles used to track fluid motion within the atmosphere. Tracers are emitted from different latitudes in the Northern Hemisphere, ranging from the equator to the pole. All tracers are impacted by the position of the jet stream, but the whether the tracer increases or decreases when the jet is in a poleward position is a strong function of where the tracers were emitted. We show that the jet stream affects variations in the north-south wind at the surface, and changes in this wind lead to the advection of air with higher or lower concentrations of tracers, depending on the latitudinal tracer gradient. Our findings may help interpret other atmospheric models that simulate pollution and greenhouse gases and the impacts of climate change on these species.

1 Introduction and Motivation

Concentrations of near-surface air pollutants and greenhouse gases exhibit large day-to-day variations, driven by a combination of variations in emissions, chemistry, and transport. Understanding the cause of this variability is paramount for interpreting measurements and trends in pollutants (e.g., Cooper et al., 2014; Dawson et al., 2014; Kerr et al., 2019) and greenhouse gases (e.g., Keppel-Aleks et al., 2011; Miller et al., 2013, 2015; Randazzo et al., 2020).

Several studies have highlighted the importance of transport in explaining the daily variability of near-surface composition. For example, daily variations of ozone (O_3) have been linked to transport-related phenomena such as horizontal and vertical advection and frontal systems (Jacob et al., 1993; Kerr et al., 2019; Porter & Heald, 2019; Kerr et al., 2020), while Keppel-Aleks et al. (2011) and Torres et al. (2019) have shown that the variability of carbon dioxide (CO_2) attributed to the prevailing synoptic- and mesoscale weather is of similar magnitude to the variability from local diurnal fluxes. Moreover, variations in the meridional, or north-south, position of the jet stream and its effect on transient atmospheric eddies and frontal zones have been linked to variability in near-

surface particulate matter (Ordóñez et al., 2019), CO_2 (Randazzo et al., 2020; Pal et al., 2020), methane (Guha et al., 2018), and O_3 (Barnes & Fiore, 2013; Shen et al., 2015; Kerr et al., 2020).

A recent study by Kerr et al. (2020) provided further support for a link between variability in the upper-level jet and surface-level O_3 but also showed substantial spatial variations in the relationship. They showed that the daily variability in surface-level O_3 during boreal summer (JJA) is significantly correlated with the meridional position of the jet across the Northern Hemisphere mid-latitudes, but the sign of the relationship differed between land and ocean (with O_3 increasing over land but decreasing over the oceans when the jet is in a poleward position). Furthermore, the O_3 -jet relationship is weak or non-existent at high and low latitudes.

The findings from the aforementioned studies raise several important questions: What mechanisms connect flow aloft to near-surface composition and variability? Why does the O₃-jet relationship vary with latitude and between land and ocean? How do species' lifetimes and source regions affect the relationship? The last question is important when considering the jet's role in the variability of greenhouse gases and surface-level particular matter whose lifetimes and source regions differ. Increases in anthropogenic greenhouse gas emissions will likely shift the mean jet latitude poleward and modulate jet speed later in the twenty-first century (Barnes & Polvani, 2013). These projected changes warrant an improved understanding of how flow aloft impacts near-surface composition, which could improve our projections of how future pollutant distributions could change.

We address these questions by performing chemical transport model (CTM) simulations of a suite of idealized tracers with differing source regions. The simulations enable us to examine how the Northern Hemisphere tracer-jet relationships vary with source region and under what condition(s) there are land-ocean or seasonal variations. Idealized tracers can aid in understanding and interpreting the impact of the jet stream on near-surface composition while avoiding the complex interplay of non-linear gas- and particle-phase chemistry and temporally- and spatially-varying precursor emissions (e.g. Orbe et al., 2016).

In Section 2, we describe the CTM simulations, reanalysis, and methodology used in this study. We document the relationship of the tracers with the jet in Section 3.1 and the impact of the jet on near-surface meridional wind in Section 3.2. We find simple balances that relate the connection of the jet stream with near-surface meridional winds to the meridional tracer gradient give a satisfying physical explanation to differences in the sign of the tracer-jet relationships (Sections 3.2-4).

2 Data and Methodology

We use the GEOS-Chem CTM (version 12.0.2) to perform our tracer simulations (Bey et al., 2001; The International GEOS-Chem User Community, 2018, October 10). GEOS-Chem is driven by assimilated meteorology from the Modern Era-Retrospective Analysis for Research and Analysis, Version 2 (MERRA-2). Three-dimensional MERRA-2 fields are input to the CTM every three hours, while surface quantities and mixing depths are provided every hour. Specifically, our configuration of GEOS-Chem follows a passive simulation described in Liu et al. (2001). We perform this simulation at 2° latitude x 2.5° longitude resolution with 72 vertical levels (~ 15 hPa spacing below 800 hPa) for 2007 - 2010, and we discard the first year (2007) for spin up.

Previous studies have demonstrated the accuracy of transport in GEOS-Chem and the assimilated meteorological product, MERRA-2, driving the CTM. Bosilovich et al. (2015) showed that magnitude of MERRA-2 zonal and meridional wind fields as well as the location of wind maxima are well-constrained by observations and other reanalyses. GEOS-Chem yields realistic mixing ratios and seasonal and latitudinal variations of other

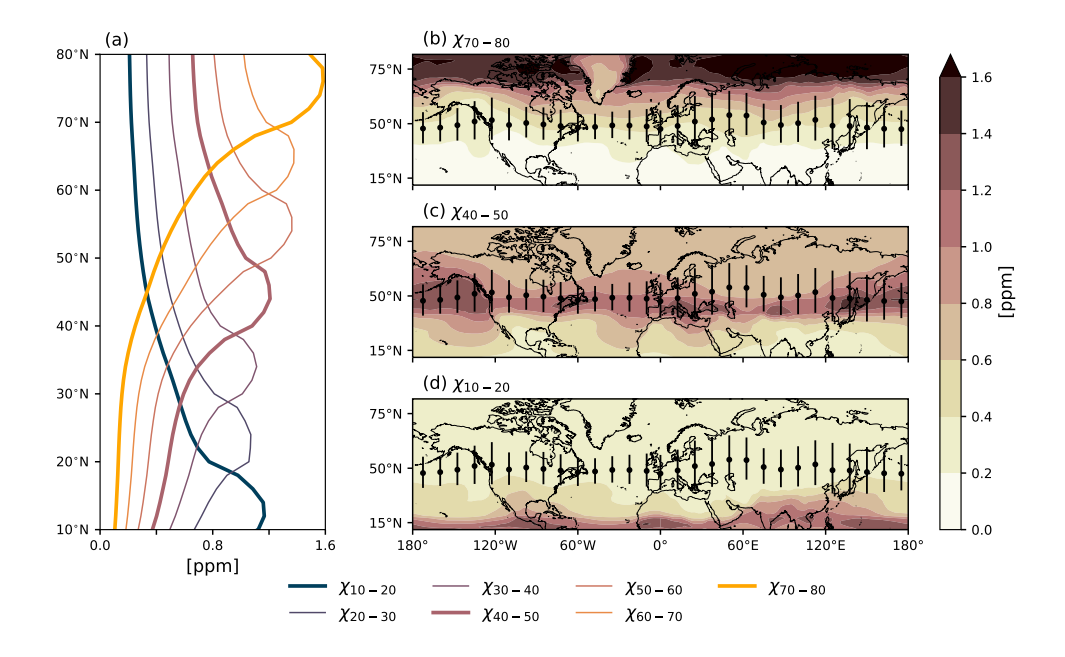


Figure 1. (a) Zonally-averaged tracer mixing ratios in JJA. (b) JJA-averaged mixing ratios of (b) χ_{70-80} , (c) χ_{40-50} , and (d) χ_{10-20} . Scatter points and vertical bars in (b)-(d) represent the mean position and variability of the jet stream in JJA, respectively. Note that the thicker lines in (a) correspond to the tracers featured in (b)-(d).

tracers such as lead and beryllium with no significant global bias (Liu et al., 2001). However, Yu et al. (2018) recently pointed out that the use of offline CTMs, such as GEOS-Chem, together with an archived assimilated meteorological product can lead to vertical transport errors due, in part, to loss of transient advection (resolved convection). While potential biases and errors are important to keep in mind, the extensive body of literature on the reliability of GEOS-Chem supports its suitability as the framework to address our research questions.

Within GEOS-Chem, we implement a suite of nine passive tracers that differ only in their source regions, which are prescribed as constant flux boundary conditions (i.e., emissions) in zonally-symmetric 10° latitudinal bands. Tracers are herein denoted $\chi_{\phi_1-\phi_2}$, where ϕ_1 is the latitude corresponding to the southern boundary of the source region and ϕ_2 is the northern boundary. All tracers decay uniformly at a loss rate of $\tau=50$ days⁻¹. Tracers with the same loss have been used in prior studies (e.g., Shindell et al., 2008; Orbe et al., 2017, 2018; Yang et al., 2019). Although not the primary focus of our analysis, we also explore how the lifetime of tracers impacts their relationship with the jet by simulating χ_{40-50} with loss rates of $\tau=5,25,100$ and 150 days⁻¹. All analyses below use daily mean near-surface (1000 – 800 hPa) tracer mixing ratios.

In addition to driving the GEOS-Chem simulations, we use MERRA-2 to characterize the meteorology responsible for tracer variability (McCarty et al., 2016; Gelaro et al., 2017). MERRA-2 is output on a global 0.5° x 0.625° grid with 72 vertical levels. Specifically, we obtain 3-hourly 1000-800 hPa meridional wind (V) and 500 hPa zonal wind (U) from MERRA-2 and average these data to daily mean values, consistent with our treatment of tracers from GEOS-Chem. The horizontal resolution differs between GEOS-Chem and MERRA-2, and we degrade the resolution of MERRA-2 to match that

of GEOS-Chem using xESMF, a universal regridder for geospatial data (Zhuang et al., 2020).

We locate ϕ_{jet} daily at each longitude by finding the latitude (restricted to 20–70°N) of maximum 500 hPa U. A simple convolution-based smoothing is applied in longitudinal space to address potential longitudinal discontinuities in the jet's position (i.e., "jumps" in the latitude of the jet) using a box-shaped function with a width of $\sim 10^{\circ}$ longitude (Barnes & Fiore, 2013; Kerr et al., 2020).

The temporal correlation between ϕ_{jet} and near-surface tracer mixing ratios or V is quantified with the Pearson product-moment correlation coefficient, indicated by r(X,Y), where X and Y are the time series of interest. We assess the significance of the correlation coefficient using the non-parametric moving block bootstrapping method, which preserves much of the temporal correlation in the time series and makes no a priori assumptions about the time series' distributions. In essence, time series X and Y are randomly reordered by sampling continuous blocks of data with length = 10 days, and r(X,Y) is thereafter recalculated. We conduct 10000 realizations of this reordering, and significance is determined with a two-tailed percentile confidence interval method at the 0.05 significance level (Wilks, 1997; Mudelsee, 2003; Wilks, 2011).

We also generate composites of tracer mixing ratios and V on days when the jet stream is poleward (PW) and equatorward (EW). The PW (EW) composite is defined locally (i.e., at each longitude) as the average value of the field of interest for days where ϕ_{jet} exceeds (is less than) the 70th (30th) percentile. We define a "positive" relationship to mean that the PW (EW) movement of the jet is associated with increased (decreased) mixing ratios or V. The opposite is true for a "negative" tracer-jet relationship.

3 Results

3.1 Relationship between the jet stream and tracers

Before we examine the tracers' relationship with the jet stream we briefly discuss the mean tracer distributions and their daily variability. Zonally-averaged tracer mixing ratios peak within their source regions and diminish to roughly half of their peak value $\pm 5^{\circ}$ outside their source regions (Figure 1a). Tracers with source regions at latitudes (ϕ) north of 60°N have higher mixing ratios within their source regions compared with tracers emitted at lower latitudes (Figure 1a), supporting an isolated Arctic lower troposphere and the "polar dome" as a barrier to transport (Law & Stohl, 2007).

Despite zonally-symmetric emissions, there are zonal variations in tracer mixing ratios (Figure 1b-d). The latitudinal range with high tracer mixing ratios (> 0.8 ppm) is larger over the ocean basins for tracers with high and mid-latitude sources (e.g., χ_{70-80} , χ_{40-50} ; Figure 1b-c). These ocean regions coincide with the Atlantic and Pacific storm tracks. High mixing ratios of tracers with source regions in the tropics (e.g., χ_{10-20}) are more diffuse over land and more restricted over the tropical ocean (Figure 1d).

Spatial variations in the tracers' daily variability (as measured by the standard deviation) are similar to spatial variations in their mean distribution, with highest variability near the tracer source region and decreasing to the north and south (not shown). Furthermore the ratio of each tracer's standard deviation to its mean is $\sim 50\%$ near the source region and diminishes to $\sim 20\%$ well outside the source region (not shown).

To examine the impact of the meridional movement of the jet on daily tracer variability, we examine composites of tracer mixing ratios when the jet is PW and EW (see Section 2). As shown in Figure 2, there is a significant tracer-jet relationship for all tracers during JJA and DJF within the mid-latitudinal range over which the jet traverses. However, the sign of the relationship hinges on the meridional gradients of the tracers

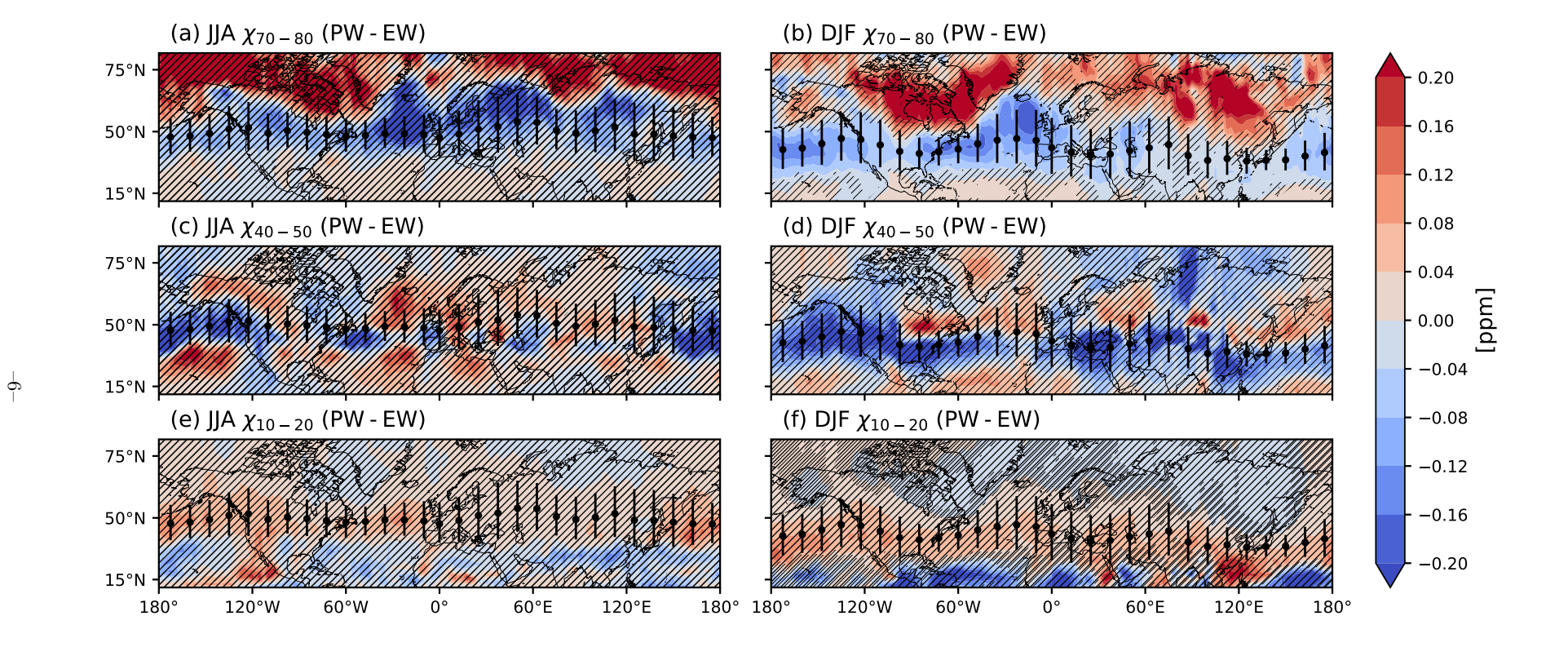


Figure 2. The difference in composites of JJA (a) χ_{10-20} , (c) χ_{40-50} , and (e) χ_{70-80} for days with a PW versus EW jet stream. Hatching denotes statistically non-significant tracer-jet correlations. Scatter points and vertical bars represent the mean position and variability of the jet stream in JJA, respectively. (b), (d), and (f) are the same as (a), (c), and (f) but for DJF.

 $(\partial\chi/\partial\phi)$. Tracers with source regions at low latitudes ($\phi<40^{\circ}N$) have a negative gradient ($\partial\chi/\partial\phi<0$) within the latitudinal range of the jet and increase in the mid-latitudes when the jet is PW (Figure 2a-b). Tracers emitted around the latitude of the jet ($40^{\circ}<\phi<60^{\circ}N$) have a spatially-varied gradient and relationship with the jet in the midlatitudes. In particular, we note the land-ocean differences in the JJA χ_{40-50} -jet relationship (Figure 2c). Tracers with source regions at high latitudes ($\phi>60^{\circ}N$) are characterized by $\partial\chi/\partial\phi>0$ in the mid-latitudes and decrease in the mid-latitudes when the jet is PW (Figure 2e-f).

Beyond the mid-latitudes and these three tracers, impact of source region on the tracer-jet relationships for all the GEOS-Chem tracers can be easily seen in the zonal mean (Figure 3a-b). The tracer-jet relationships all exhibit an oscillatory pattern, but tracers with source regions south of the range of the jet are positively correlated with the jet in the mid-latitudes and are flanked by negative correlations (although generally non-significant) outside the mid-latitudes. Tracers with source regions north of the jet have a negative correlation with the jet in the mid-latitudes and a positive, but non-statistically significant, correlation outside the mid-latitudes (Figure 3a-b).

The variations in tracer mixing ratios related to the meridional oscillations of the jet are a sizable fraction of the overall daily tracer variability discussed earlier in this section. For example, the ratios of the jet-associated variations in χ_{10-20} , χ_{40-50} , and χ_{70-80} to the overall variability (standard deviation) zonally-averaged over the mid-latitudes $(40^{\circ} < \phi < 60^{\circ}\text{N})$ are 58%, 35%, and 47%, respectively.

In a gross sense, the relationship between the jet stream and our tracers does not change in DJF compared to JJA, but further inspection suggests that there are nuanced differences in the tracer-jet relationships (Figure 2). For example, the change in mid-latitude mixing ratios of χ_{40-50} due to the meridional movement of the jet is varied in sign and strength during JJA, while the DJF change is largely negative (Figure 3b-c).

We also evaluate how tracer lifetime impacts the tracer-jet relationships within GEOS-Chem by simulating χ_{40-50} with loss rates ranging from 5 to 150 days (Section 2). The relationship of the jet with χ_{40-50} for loss rates ≥ 25 days⁻¹ are virtually identical in sign, strength, and significance to χ_{40-50} with the 50 day⁻¹ loss rate discussed elsewhere in this study (not shown). Even χ_{40-50} with a 5 day lifetime has a significant relationship with the jet in regions with intense flow aloft (i.e., the Pacific and Atlantic storm tracks). Thus, the jet is an important source of variability for surface-level trace species spanning a wide range of lifetimes.

3.2 Mechanisms

The analysis presented in Section 3.1 has shown that a large fraction of daily tracer variability is related to meridional movement of the jet but does not show the mechanism(s) involved or why the signs of the tracer-jet relationships varies. Kerr et al. (2020) suggested that the jet stream affects surface-level O_3 by altering the near-surface meridional flow (V). We test this hypothesis using our suite of tracers. We first examine the V-jet relationship and then how this impacts the tracers.

Figure 3c indicates that southerly flow increases in the mid-latitudes (around the latitudinal range of the jet stream) when the jet is PW during JJA and DJF; however, it does not show the magnitude. As is shown in Figure 4a-b, V increases over 5 m/s in parts of the mid-latitudes when the jet is PW. This stands in sharp contrast to time-averaged V, which is generally weak (-2 < V < 2 m/s) over the vast majority of the mid-latitudes. It is exceedingly rare for time-averaged V to have the same magnitude changes in V linked to the jet (contours in Figure 4a-b). Outside the mid-latitudes, the relationship between V and ϕ_{jet} is largely non-significant and weak (Figures 3c, 4a-b).

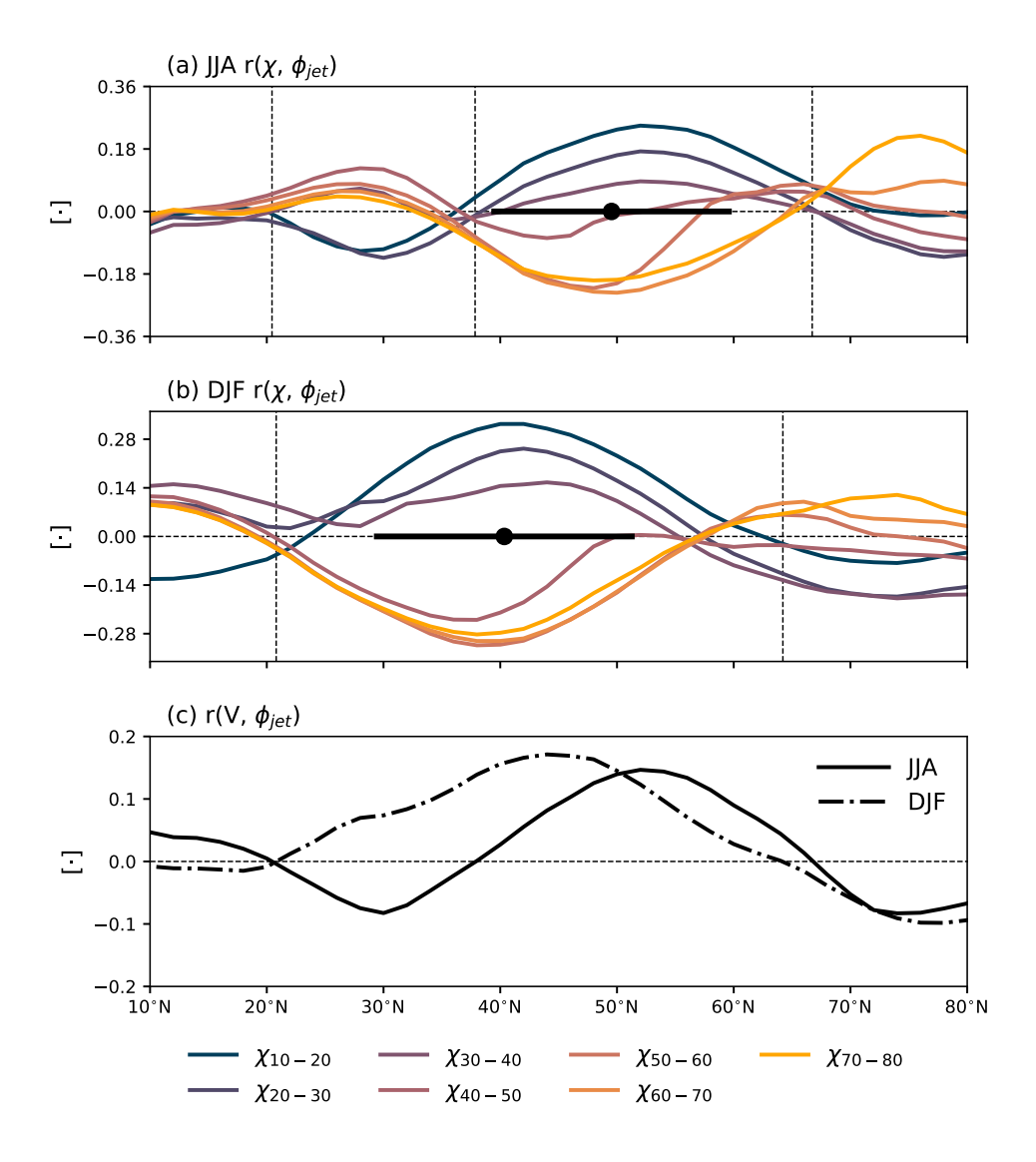


Figure 3. An illustration of how ϕ_{jet} impacts near-surface V and tracers. (a) The JJA zonally-averaged correlation between ϕ_{jet} and individual tracers (colors) and the mean position and and variability of the jet stream (scatter point and horizontal bars). (b) same as (a) but for DJF. (c) Zonally-averaged $r(V,\phi_{jet})$. Dashed vertical lines in (a)-(b) denote the latitudes where $r(V,\phi_{jet})=0$ for each season. Dashed horizontal lines separate positive from negative correlations.

The V-jet relationship is not zonally-symmetric (Figure 4a-b). For example, the JJA V-jet relationship is negative over the mid-latitude oceans on the windward shores of the continents but is positive over the mid-latitude continents and the leeward shores (Figure 4a).

238

239

240

241

243

244

245

In the zonal mean, the latitudes, or nodes, where $r(\chi, \phi_{jet}) = 0$ are well-aligned with the latitudes where the jet stream and V are not correlated (Figure 3). The only node where $r(V, \phi_{jet}) = 0$ does not coincide with $r(\chi, \phi_{jet}) = 0$ occurs during DJF north of the jet (Figure 3b). In this case, the latitude where $r(V, \phi_{jet}) = 0$ lies north of $r(\chi, \phi_{jet}) = 0$ by $\sim 5^{\circ}$, and other processes could be important for the tracer-jet re-

lationships in this region and season. These results support Kerr et al. (2020) and provide strong evidence linking the tracer-jet relationships to (1) the source region of the tracers and (2) the V-jet relationship (Figure 3).

The jet-induced change in V modifies meridional tracer advection (i.e., $-V \cdot \partial \chi/\partial \phi$). Thus, the impact of a given change in V is expected to depend on the local tracer gradients. If $\partial \chi/\partial \phi$ is weak, then smaller tracer changes are expected compared with locations with stronger $\partial \chi/\partial \phi$. It also follows that the same change in V operating over $\partial \chi/\partial \phi < 0$ versus $\partial \chi/\partial \phi > 0$ would result in changes of tracer mixing ratios with different signs. Given this, we postulate that the expected sign of the tracer-jet relationships $(E[r(\chi,\phi_{jet})])$ shown in Figures 2-3 can be approximated by:

$$E[r(\chi, \phi_{jet})] \sim -r(V, \phi_{jet}) \cdot \frac{\partial \chi}{\partial \phi}.$$
 (1)

In practice, this balance implies that the anomalous southerly flow in the mid-latitudes that accompanies a PW-shifted jet $(r(V, \phi_{jet}) > 0)$ will advect higher tracer mixing ratios from lower latitudes if $\partial \chi/\partial \phi < 0$, yielding a positive expected tracer-jet relationship (i.e., $E[r(\chi, \phi_{jet})] > 0$).

The application of Equation 1 does not capture the sign of the χ_{40-50} -jet relationship in the vicinity of the Atlantic and Pacific storm tracks (Figure 4c-d), and this is the case for other tracers as well (not shown). Since our tracer mixing ratios are roughly zonally-symmetric (Figure 1b-d), the effect of changes in the zonal wind are negligible to first order. However, the jet stream exerts an influence on near-surface U (Woollings et al., 2010), especially near the exit region of the these storm tracks. To account for this, future studies could consider the impact of both the V-jet and U-jet relationships.

The zonal variations in the tracer-jet relationships shown above could stem from zonal variations in the response of V to the movement of the jet or zonal variations in the tracer gradients. To explore this, we have isolated the terms in Equation 1 by separately fixing each to its zonal mean value and thereafter recalculating $E[r(\chi,\phi_{jet})]$ to gauge which exerts a stronger influence on the tracer-jet relationships (not shown). Recalculating Equation 1 with $\partial\chi/\partial\phi$ fixed to its zonal mean value and $r(V,\phi_{jet})$ varying as in Figure 4a-b yields expected tracer-jet relationships with zonal variations that resemble the relationships shown in Figure 4c-d. This sensitivity test together with the analysis performed in Figure 4c-d confirm spatiotemporal variations in the V-jet relationship are the most important factor in explaining the tracer-jet coupling, followed by the latitudinal tracer gradient.

All of our analyses presented in this manuscript have also been repeated with tropospheric ($1000-200~\mathrm{hPa}$) column-averaged tracer mixing ratios. We find that the role of the V-jet relationship on explaining variations in tracer column abundances remains unchanged.

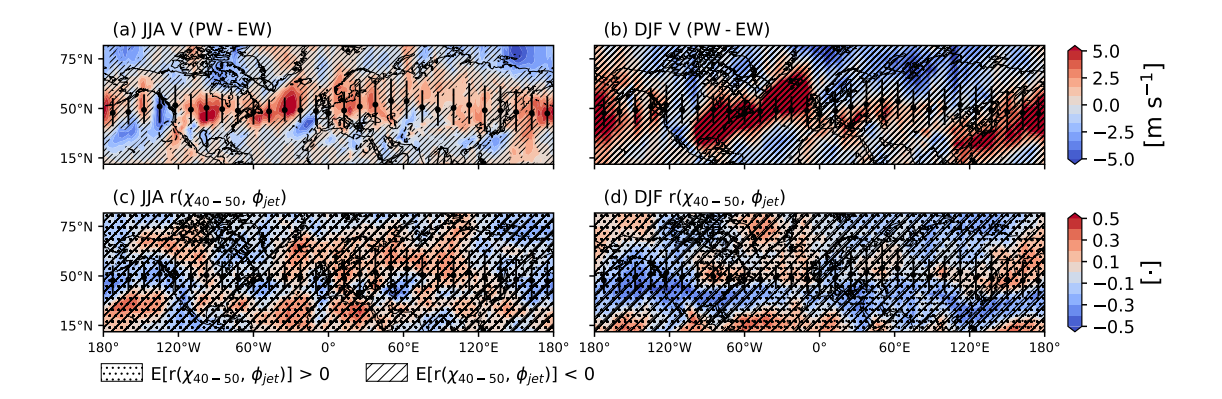


Figure 4. (a-b) Differences in composites of V for days with a PW versus EW jet stream (colors). Time-averaged V is illustrated for 5 m/s (solid black contour) and -5 m/s (dashed black contour). Hatching denotes statistically non-significant V-jet correlations. (c-d) The correlation coefficient calculated between χ_{40-50} and ϕ_{jet} (colors). As denoted in the legend beneath (c), stippling and hatching show the expected sign of the correlation, $E[r(\chi_{40-50}, \phi_{jet})]$, determined using Equation 1. Scatter points and vertical bars in all subplots represent the mean position of and variability of the jet stream, respectively.

4 Conclusions

This study demonstrates that the daily variability of the position of the jet stream has a strong influence on near-surface tracer mixing ratios and meridional flow within the seasonally-dependent range of the jet.

The sign of the tracer-jet relationships varies with tracer meridional gradients due to the impact that position of the jet has on near-surface meridional flow (Figures 2, 3a-b). Tracers with a negative gradient within the latitudinal range of the jet have positive tracer-jet relationships in the mid-latitudes, while the opposite is true for tracers with positive gradients within the jet's range. Tracers whose source regions are within the range of the jet have spatially-varied gradients and therefore a zonally-asymmetric relationship with the jet in the mid-latitudes. This mechanism is able to explain (1) the origin of the land-ocean differences and (2) why seasonal differences exist. These results not only help us interpret our idealized tracers but also lend insights to other species (e.g., O_3 ; Kerr et al., 2020).

Contemporaneous studies have found that variations in meteorology can explain a substantial portion of total column observations, comparable to the impact of regional variations in surface fluxes (e.g., Keppel-Aleks et al., 2011). The robustness of our results to both near-surface and total column mixing ratios may be useful for interpreting variations in the total column measurements commonplace among satellite products. Differentiating whether patterns in satellite observations are due to transport versus variations in surface fluxes may help explain differences in trace gas distributions due to large-scale transport. Moreover, inverse modeling techniques, which often employ column abundances to infer the surface fluxes of trace gases, may benefit from the improved insight presented herein regarding a major source of trace gas variability.

Though we have considered only idealized tracers with zonally-uniform emissions, our results may extend to a host of species with varied lifetimes, as long as their lifetimes sufficiently-long to undergo synoptic-scale transport. Future studies should test this and also explore how zonally-asymmetric emissions affect their relationship with the jet.

Our study has documented a major driver of near-surface composition variability (i.e., transport associated with the jet stream) and linked this driver with the location of emissions. This finding is especially relevant as models of future climate predict that the jet stream will migrate north (e.g., Barnes & Polvani, 2013), increasing poleward transport of air pollution and greenhouse gases via its regulation of the near-surface meridional flow. Expected changes in the jet together with a redistribution of anthropogenic emissions from the mid-latitudes (developed nations) to low latitudes (developing nations) (Zhang et al., 2016) necessitates that the role of the jet stream, the associated meridional wind response, and the location of emissions should be a deliberate consideration of future work on chemistry-climate connections.

Acknowledgments

This work is supported by NASA's Atmospheric Composition Modeling and Analysis Program (Grant No. NNX17AI31G) and NSF's Integrative Graduate Education and Research Traineeship Program (Grant No. 1069213). GEOS-Chem simulations were run on the Maryland Advanced Research Computing Center (MARCC). NASA's Global Modeling and Assimilation Office and Goddard Earth Sciences Data and Information Services Center (GES DISC) provided and disseminated the MERRA-2 data used in this study, specifically the inst3_3d_asm_Np collection (Global Modeling and Assimilation Office (GMAO), 2015).

References

- Barnes, E. A., & Fiore, A. M. (2013). Surface ozone variability and the jet position: Implications for projecting future air quality. *Geophys. Res. Lett.*, 40(11), 2839–2844. doi: 10.1002/grl.50411
- Barnes, E. A., & Polvani, L. (2013). Response of the midlatitude jets, and of their variability, to increased greenhouse gases in the CMIP5 models. *J. Clim.*, 26(18), 7117–7135. doi: 10.1175/JCLI-D-12-00536.1
 - Bey, I., Jacob, D. J., Yantosca, R. M., Logan, J. A., Field, B. D., Fiore, A. M., et al. (2001). Global modeling of tropospheric chemistry with assimilated meteorology: Model description and evaluation. *J. Geophys. Res. Atmos.*, 106 (D19), 23073–23095. doi: 10.1029/2001jd000807
- Bosilovich, M., Akella, S., Coy, L., Cullather, R., Draper, C., Gelaro, R., et al. (2015). *MERRA-2: Initial evaluation of the climate, NASA/TM-2015-104606* (Vol. 43).
- Cooper, O. R., Parrish, D. D., Ziemke, J., Balashov, N. V., Cupeiro, M., Galbally, I. E., et al. (2014). Global distribution and trends of tropospheric ozone: An observation-based review. *Elem. Sci. Anth.*, 2, 000029. doi: 10.12952/journal.elementa.000029
- Dawson, J. P., Bloomer, B. J., Winner, D. A., & Weaver, C. P. (2014). Understanding the meteorological drivers of U.S. particulate matter concentrations in a changing climate. *Bull. Amer. Meteor. Soc.*, 95(4), 521–532. doi: 10.1175/bams-d-12-00181.1
- Gelaro, R., McCarty, W., Suárez, M. J., Todling, R., Molod, A., Takacs, L., et al. (2017). The Modern-Era Retrospective Analysis for Research and Applications, Version 2 (MERRA-2). *J. Clim.*, 30(14), 5419–5454. doi: 10.1175/JCLI-D-16-0758.1
- Global Modeling and Assimilation Office (GMAO). (2015).

 MERRA-2 inst3_3d_asm_Np:3d,3-Hourly,Instantaneous,PressureLevel,Assimilation,Assimilated Meteorological Fields V5.12.4. Greenbelt, MD,
 USA. (Last accessed: 25 September 2019) doi: 10.5067/QBZ6MG944HW0
 - Guha, T., Tiwari, Y. K., Valsala, V., Lin, X., Ramonet, M., Mahajan, A., . . . Kumar, K. R. (2018). What controls the atmospheric methane sea-

sonal variability over India? Atmos. Environ., 175, 83–91. doi: 10.1016/j.atmosenv.2017.11.042

- Jacob, D. J., Logan, J. A., Gardner, G. M., Yevich, R. M., Spivakovsky, C. M., Wofsy, S. C., et al. (1993). Factors regulating ozone over the United States and its export to the global atmosphere. J. Geophys. Res., 98(D8), 14817. doi: 10.1029/98jd01224
 - Keppel-Aleks, G., Wennberg, P. O., & Schneider, T. (2011). Sources of variations in total column carbon dioxide. *Atmos. Chem. Phys.*, 11(8), 3581–3593. doi: 10.5194/acp-11-3581-2011
 - Kerr, G. H., Waugh, D. W., Steenrod, S. D., Strode, S. A., & Strahan, S. E. (2020). Surface ozone-meteorology relationships: Spatial variations and the role of the jet stream. Submitted to J. Geophys. Res. Atmos..
 - Kerr, G. H., Waugh, D. W., Strode, S. A., Steenrod, S. D., Oman, L. D., & Strahan, S. E. (2019). Disentangling the drivers of the summertime ozone-temperature relationship over the United States. J. Geophys. Res., 124 (19), 10503–10524. doi: 10.1029/2019jd030572
 - Law, K. S., & Stohl, A. (2007). Arctic air pollution: Origins and impacts. *Science*, 315 (5818), 1537–1540. doi: 10.1126/science.1137695
 - Liu, H., Jacob, D. J., Bey, I., & Yantosca, R. M. (2001). Constraints from ²¹⁰Pb and ⁷Be on wet deposition and transport in a global three-dimensional chemical tracer model driven by assimilated meteorological fields. *J. Geophys. Res. Atmos.*, 106 (D11), 12109–12128. doi: 10.1029/2000jd900839
 - McCarty, W., Coy, L., Gelaro, R., Huang, A., Merkova, D., Smith, E. B., et al. (2016). *MERRA-2 input observations: Summary and assessment* (Technical Report Series on Global Modeling and Data Assimilation, Volume 46). Greenbelt, MD, USA: National Aeronautics and Space Administration.
 - Miller, S. M., Hayek, M. N., Andrews, A. E., Fung, I., & Liu, J. (2015). Biases in atmospheric CO₂ estimates from correlated meteorology modeling errors. Atmos. Chem. Phys., 15(5), 2903–2914. doi: 10.5194/acp-15-2903-2015
 - Miller, S. M., Wofsy, S. C., Michalak, A. M., Kort, E. A., Andrews, A. E., Biraud, S. C., et al. (2013). Anthropogenic emissions of methane in the United States. *Proc. Natl. Acad. Sci. U.S.A.*, 110(50), 20018–20022. doi: 10.1073/pnas.1314392110
 - Mudelsee, M. (2003). Estimating Pearson's correlation coefficient with bootstrap confidence interval from serially dependent time series. *Math. Geol.*, 35(6), 651–665. doi: 10.1023/b:matg.0000002982.52104.02
 - Orbe, C., Waugh, D. W., Newman, P. A., & Steenrod, S. (2016). The transit-time distribution from the Northern Hemisphere midlatitude surface. *J. Atmos. Sci.*, 73(10), 3785–3802. doi: 10.1175/jas-d-15-0289.1
 - Orbe, C., Waugh, D. W., Yang, H., Lamarque, J.-F., Tilmes, S., & Kinnison, D. E. (2017). Tropospheric transport differences between models using the same large-scale meteorological fields. *Geophys. Res. Lett.*, 44 (2), 1068–1078. doi: 10.1002/2016gl071339
 - Orbe, C., Yang, H., Waugh, D. W., Zeng, G., Morgenstern, O., Kinnison, D. E., et al. (2018). Large-scale tropospheric transport in the Chemistry-Climate Model Initiative (CCMI) simulations. *Atmos. Chem. Phys.*, 18(10), 7217–7235. doi: 10.5194/acp-18-7217-2018
- Ordóñez, C., Barriopedro, D., & García-Herrera, R. (2019). Role of the position of the North Atlantic jet in the variability and odds of extreme PM₁₀ in Europe. *Atmos. Environ.*, 210, 35–46. doi: 10.1016/j.atmosenv.2019.04.045
- Pal, S., Davis, K. J., Lauvaux, T., Browell, E. V., Gaudet, B. J., et al. (2020). Observations of greenhouse gas changes across summer frontal boundaries in the Eastern United States. *J. Geophys. Res. Atmos.*, 125(5). doi: 10.1029/2019jd030526
 - Porter, W. C., & Heald, C. L. (2019). The mechanisms and meteorological drivers of

the ozone-temperature relationship. Atmos. Chem. Phys., 13367-13381. doi: 10 .5194/acp-2019-140

- Randazzo, N. A., Michalak, A. M., & Desai, A. R. (2020). Synoptic meteorology explains temperate forest carbon uptake. *J. Geophys. Res. Biogeosci.*, 125(2). doi: 10.1029/2019jg005476
- Shen, L., Mickley, L. J., & Tai, A. P. K. (2015). Influence of synoptic patterns on surface ozone variability over the eastern United States from 1980 to 2012. *Atmos. Chem. Phys.*, 15(19), 10925–10938. doi: 10.5194/acp-15-10925-2015
- Shindell, D. T., Chin, M., Dentener, F., Doherty, R. M., Faluvegi, G., Fiore, A. M., et al. (2008). A multi-model assessment of pollution transport to the Arctic. *Atmos. Chem. Phys.*, 8(17), 5353–5372. doi: 10.5194/acp-8-5353-2008
- The International GEOS-Chem User Community. (2018, October 10). geoschem/geos-chem: Geos-chem 12.0.2 release (Version 12.0.2). Zenodo. Retrieved from http://doi.org/10.5281/zenodo.1455215
- Torres, A. D., Keppel-Aleks, G., Doney, S. C., Fendrock, M., Luis, K., Mazière, M. D., et al. (2019). A geostatistical framework for quantifying the imprint of mesoscale atmospheric transport on satellite trace gas retrievals. *J. Geophys. Res. Atmos.*, 124 (17-18), 9773–9795. doi: 10.1029/2018jd029933
- Wilks, D. S. (1997). Resampling hypothesis tests for autocorrelated fields. *J. Clim.*, 10(1), 65-82. doi: $10.1175/1520-0442(1997)010\langle0065:\text{rhtfaf}\rangle2.0.\text{co};2$
- Wilks, D. S. (2011). Statistical methods in the atmospheric sciences. Amsterdam; Boston: Elsevier Academic Press.
- Woollings, T., Hannachi, A., & Hoskins, B. (2010). Variability of the North Atlantic eddy-driven jet stream. Q. J. R. Meteorol. Soc., 136 (649), 856–868. doi: 10.1002/qj.625
- Yang, H., Waugh, D. W., Orbe, C., Zeng, G., Morgenstern, O., Kinnison, D. E., et al. (2019). Large-scale transport into the Arctic: The roles of the midlatitude jet and the Hadley cell. *Atmos. Chem. Phys.*, 19(8), 5511–5528. doi: 10.5194/acp-19-5511-2019
- Yu, K., Keller, C. A., Jacob, D. J., Molod, A. M., Eastham, S. D., & Long, M. S. (2018). Errors and improvements in the use of archived meteorological data for chemical transport modeling: An analysis using GEOS-Chem v11-01 driven by GEOS-5 meteorology. *Geosci. Model Dev.*, 11(1), 305–319. doi: 10.5194/gmd-11-305-2018
- Zhang, Y., Cooper, O. R., Gaudel, A., Thompson, A. M., Nédélec, P., Ogino, S.-Y., & West, J. J. (2016). Tropospheric ozone change from 1980 to 2010 dominated by equatorward redistribution of emissions. *Nat. Geosci.*, 9(12), 875–879. doi: 10.1038/ngeo2827
- Zhuang, J., Dussin, R., Jüling, A., & Rasp, S. (2020). Jiaweizhuang/xesmf: v0.3.0 adding esmf.locstream capabilities. Zenodo. Retrieved from https://zenodo.org/record/1134365 doi: 10.5281/ZENODO.1134365